# High Performance Mach Zehnder Based Silicon Optical Modulators

David J. Thomson, Frederic Y. Gardes, S. Liu, H. Porte, L. Zimmermann, J-M Fedeli, Y. Hu, M. Nedeljkovic, X. Yang, P. Petropoulos and G. Z. Mashanovich

***Abstract*—Silicon photonics is poised to revolutionise several data communication applications. The development of high performance optical modulators formed in silicon is essential for the technology to be viable. In this paper we review our recent work on carrier depletion silicon Mach Zehnder based optical modulators which have formed part of the work within the UK Silicon Photonics and HELIOS projects, as well as including some recent new data. A concept for the self-aligned formation of the pn junction which is flexible in the capability to produce a number of device configurations is presented. This process is key in having performance repeatability, a high production yield and large extinction ratios. Experimental results from devices which are formed though such processes are presented with operation up to and beyond 40Gbit/s. The potential for silicon photonics to fulfil longer haul applications is also explored in the analysis of the chirp produced from these devices and the ability to produce large extinction ratios at high speed. It is shown that the chirp produced with the modulator operated in dual drive configuration is negligible and that a 18dB dynamic modulation depth is obtainable at a data rate of 10Gbit/s.**

***Index Terms*—Silicon, Silicon Photonics, Optical Modulator, Mach Zehnder, Chirp.**

## I. Introduction

Over the previous decade silicon photonics has emerged as an attractive technology base in which to form high photonic components and circuits. Motivated by the prospects of low cost production and integration with CMOS, which can also offer enhanced functionality silicon photonics has attracted significant research effort worldwide. This has resulted in rapid improvements in component performance and integration techniques which have opened up the technology to a number of different applications. The silicon optical modulator which performs the function of writing electrical data onto an optical carrier is a prime example of the development rate of silicon photonics. Performances have gone from the first proposed designs for 1GHz modulation a decade ago [1] to modulator at data rates in excess of 40Gbit/s [2,3]. Applications for silicon photonics have focused on short reach links with some products already emerging in the area of active optical cables [4]. The technology is a good match in this case since the cost is the key driver and performance requirements are much less stringent than for the long haul links typically associated with photonics. Longer reach photonics links are currently served by high performance components formed in more traditional photonics materials such as $LiNbO_3$ or III-V compounds such as InP. The performance of components fabricated in such materials are typically far superior to those formed in silicon. However, with the rapid emergence of silicon photonics, performance of silicon devices is improving dramatically. This focus on short reach applications has driven attention away from the analysis of some of the performance requirements when transmitting optical data over long distances. Chirp is one characteristic that becomes increasingly important with the reach of the data link, yet to date it has received relatively little investigation in silicon optical modulators [5-7]. Furthermore for the short reach links only modest extinction ratios are required. Generally the modulation depth required increases with the length of link. Commercial $LiNbO_3$ modulators typically have extinction ratios in excess of 13dB [8, 9]. To date there have very few demonstrations of extinction ratios in excess of 10dB in silicon based modulators[7, 10].

In this paper we provide a review of our recent work on carrier depletion based silicon Mach-Zehnder modulators (MZM) which has been performed within the UK Silicon Photonics (UKSP) and HELIOS projects, and we provide some new data that has recently been recorded. Two different phase modulator designs are presented, both formed using different variants of the self-aligned pn junction process. The first, formed in 220nm overlayer SOI has demonstrated operation up to 50Gbit/s [2] and at 40Gbit/s with a large extinction ratio. The second formed in 400nm overlayer SOI has demonstrated 40Gbit/s modulation for both TE and TM polarisations and has the potential for polarisation independent operation. The prospects for silicon optical modulator to be employed for longer haul application is also explored in the investigation of the chirp and the ability to achieve a large extinction ratio. We demonstrate that with dual-drive

Manuscript received (current date), 2013. The research leading to these results has received funding from the European Community's Seventh Framework Programme (FP7/2007-2013) under grant agreement n° 224312 HELIOS and from the EPSRC in the UK to support the UK Silicon Photonics project.

D. J. Thomson, F. Y. Gardes, S. Liu, Y. Hu, M. Nedeljkovic, X. Yang, P. Petropoulos, G. Z. Mashanovich and G. T. Reed are with the Optoelectronics Research Centre, University of Southampton, Southampton, Hampshire, UK, SO17 1BJ. (d.thomson@soton.ac.uk).

H. Porte is with *Photline Technologies, 16 rue Jouchoux, 25000 Besancon, France*

L. Zimmermann is with *IHP, Im Technologiepark 25, 15236 Frankfurt (Oder), Germany*

J-M Fedeli is with *CEA, LETI, Minatec, CEA-Grenoble, 17 rue des Martyrs, F-38054 GRENOBLE cedex 9, France*

operation the chirp produced is negligible. An extinction ratio of 18dB is also presented at a data rate of 10Gbit/s.

## II. Modulator Designs and Self-Aligned Fabrication

The majority of optical modulators formed in silicon are based upon the plasma dispersion effect where a change in the densities of free electrons and holes causes a change in the materials refractive index [11, 12]. The depletion of these carriers from a pn junction positioned such that it interacts with the propagating light is an approach that balances fabrication complexity, performance and CMOS compatibility. This technique had resulted in some of the most successful devices demonstrated in recent years and is the approach that has been followed in this work.

The position of the pn junction is critical to the device performance with the resultant overlap of the depletion region with the optical mode governing the phase efficiency and having an effect on the optical loss. A concept that we have developed within our work is the ability to accurately position the junction using a self-aligned fabrication process. Using this approach we can reduce performance variations caused by process tolerances. This has several benefits. Firstly device yield will be increased which will in turn allow for the chip cost to be kept low. Furthermore, costs can also be reduced since older generation fabrication tools with lower alignment accuracy can be used. Secondly when the phase modulator is used in a Mach-Zehnder Interferometer (MZI) structure it will allow the losses in the two arms to be balanced with greater accuracy providing a larger extinction ratio. Finally, with dual drive operation the matched phase modulation performance in either arm will allow for the chirp of the device to be minimised.

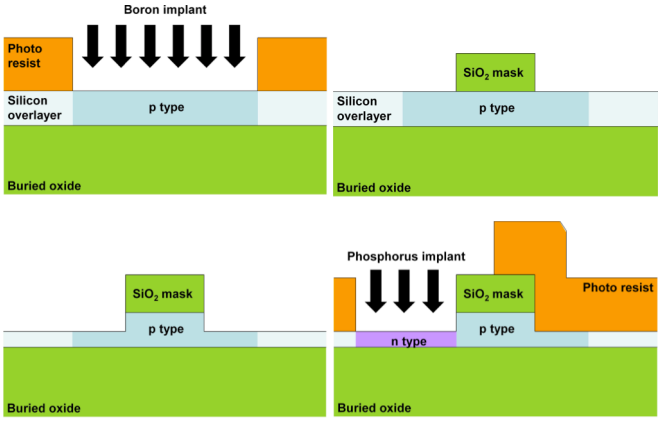


Fig.1. Diagram showing the self-aligned formation of the pn junction. Firstly the active region is doped p type (top left). A silicon dioxide layer is the deposited and patterned with the waveguide design (top right). This patterned silicon dioxide layer is then used as a hard mask through which to etch the waveguides (bottom left). Finally the silicon dioxide hard mask is used together with a photoresist window to define the phosphorus implantation region [13].

The basic concept of the self- aligned process is shown in figure 1. The active region is first doped p type by implanting boron ions though a window defined by photolithography. A silicon dioxide layer is then deposited and patterned with the waveguide design. This patterned layer is then used firstly as a hard mask through which to etch the optical waveguides. After etching the waveguides the hard mask is retained and used in combination with a photoresist layer to guide a phosphorus implant. Since either the hard mask or photoresist alone are designed to be sufficiently thick to block the implanted phosphorus ions the edge of the photoresist window can be positioned anywhere on the waveguide and the junction will always reside at the waveguide edge. A low alignment accuracy is therefore required (±200nm). The remainder of the device features are formed using CMOS compatible process steps. A cross-sectional diagram of the resultant device formed with this basic process is shown in figure 2.

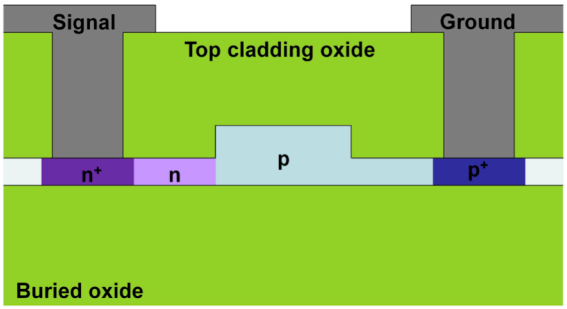


Fig. 2. Cross sectional diagram of the phase modulator formed with this simple self-aligned process [13].

As can be seen in figure 2, the pn junction is positioned in line with the edge of the waveguide. This not the natural position for the junction since it does not coincide with the core of the optical mode. In order to achieve efficient modulation with such a configuration the doping concentrations should be arranged such that the depletion extends mainly into the waveguide during reverse bias conditions. This can be achieved by having a larger n type concentration than p type. In the first variant of our design the p type density is 3e17.cm$^{-3}$ and the n type 1.5e18.cm$^{-3}$.

The waveguide dimensions are 220nm height, 400nm width and 100nm slab height. The separations between the highly doped regions and the waveguide edge are 500nm (n+) and 450nm (p+). Holes are etched through a 1 micrometer thick silicon dioxide top cladding layer down to the highly doped regions in order to form ohmic contacts to the device electrodes. Coplanar waveguide electrode are used to drive the device at high speed. An electrode thickness of 1.3um has been selected to allow for a large electrode bandwidth. The phase modulators are inserted into MZI's to convert the phase modulation into intensity modulation. Low loss multimode interference structures (MMI's) with accurate splitting ratio are used to split and combine the light from the MZI arms [14]. To simplify the characterisation the MZI have been configured to be asymmetric where one arm is 180um longer than the other. This gives a periodic spectral response as shown in figure 3, which are the results taken from a MZI with 3.5mm phase shifters. To allow dual drive operation and to balance the losses identical phase modulators are put in both MZI arms. When a reverse bias is applied to one of the arms the phase shift produced shifts the spectral response as shown in figure 3. The shift in the response relative to the free spectral range (FSR) can be used to accurately calculate the phase shift. Figure 3 demonstrates a passive extinction ratio of

around 30dB and a DC extinction ratio in excess of 25dB when 6V is applied to one arm. The modulation efficiency is measured to be approximately 2.7V.cm. Phase modulation efficiencies as low as 2.3V.cm have been demonstrated with slightly different doping configurations (spectral response shown in figure 13). The optical loss of the phase modulator relative to a waveguide of the same length is ~15dB. This comprises a phase modulator loss of 4dB/mm and an MMI loss of 0.5dB.

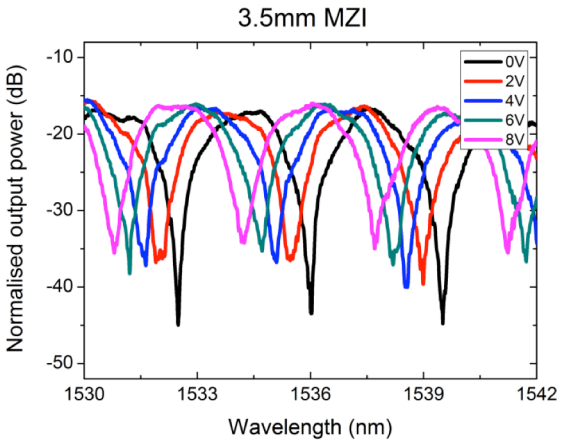


Fig. 3. Spectral response of the asymmetric MZI with 3.5mm phase shifters with different DC bias voltages applied to the phase modulator in one of the MZI arms.

The phase modulator loss results mainly from the proximity of the p+ and n+ regions to the waveguide. Our analysis suggests that these have diffused closer to the waveguide than targeted during fabrication. A loss of approximately 1.6dB/mm was expected from simulation. High speed performance has been analysed by applying a 40Gbit/s electrical PRBS data stream amplified to 6.5V peak to peak to the device with the optical output eye diagram monitored. The PRBS signal was generated using a Centellax TG1P4A source and amplified to 6.5V peak to peak using a Centellax OA4MVM3 amplifier. High speed ground-signal ground (GSG) probes were used to both launch the signal on the chip and to apply the 50Ω termination at the end of the electrode.

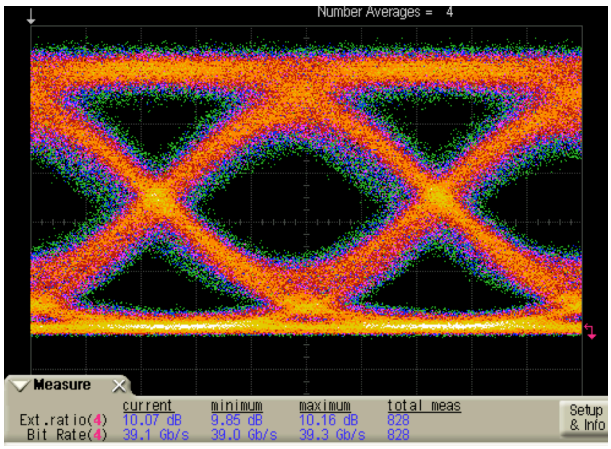


Fig. 4. 40Gbit/s operation of the MZI with 3.5mm phase shifters. The device is operated at quadrature with a 6.5V peak to peak drive voltage [13].

Figure 4 shows the optical output eye diagram from the MZI obtained using an Agilent 86100C digital communications analyser (DCA) with 86116C Opt 40 optical head. An extinction ratio of 10dB is obtained at the quadrature operating point. If the device was driven in dual drive configuration with 2V peak to peak inputs (Similar to using a 4V peak to peak input in single drive configuration) an extinction ratio of approximately 7dB would be expected [13] demonstrating the potential for the modulators use in low drive voltage applications. A MZI with 1mm phase shifters has also been tested at 50Gbit/s [2]. After accounting for EDFA noise an extinction ratio of 3dB is obtained. The device is operated at a point with slightly more loss than at quadrature resulting in a loss of approximately 7.4dB. The optical loss of the device can be improved simply by increasing the separation of the highly doped regions from the waveguide. This has been demonstrated in a separate fabrication run of the same device. The separation between the n+ and p+ regions and the waveguide in this case was increased to 600nm and 500nm respectively. This resulted in a loss of just 1.1dB respectively. Note that a slightly different doping recipe was used for the waveguide which resulted in a phase efficiency if 2.9V.cm. The separations of the highly doped regions from the waveguide are normally selected to trade-off device speed and loss. Using a greater separation from the waveguide decreases interaction with the optical mode and therefore reduces optical loss. An increased access resistance to the devices also results which causes a reduction in the intrinsic bandwidth. Although the separations have been increased high speed operation at 20Gbit/s and 30Gbit/s has been demonstrated as shown in figure 5.

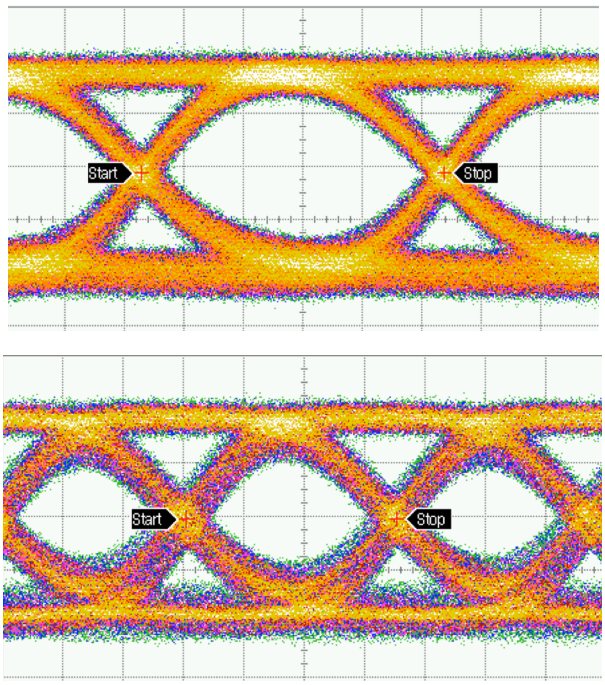


Fig. 5. Operation of the phase modulator with larger separation between the waveguide and the highly doped regions at data rates of 20Gbit/s (top) and 30Gbit/s (bottom).

In this case the device speed is limited not by the semiconductor section of the device but by the electrodes

which were fabricated in much thinner metal (580nm) than used previously.

Although the phase modulation efficiency produced is respectable compared with the state of the art our analysis suggests that for similar optical losses the modulation efficiency can be increased by moving the junction slightly inside the waveguide. This can be achieved with the self-aligned junction formation retained by using angled implantations as shown in figure 6. By controlling the angle, energy and dose of the phosphorus implant it is possible to position the pn junction at whatever position required. Other techniques such as plasma immersion or dopant diffusion can also be employed to a similar affect.

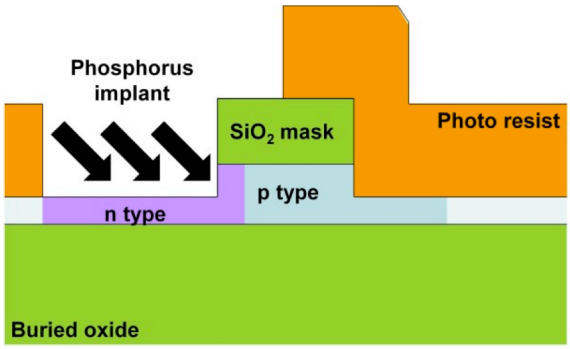


Fig. 6. Diagram showing how the pn junction can be positioned inside the waveguide using the same self-aligned process concept by using an angled phosphorus implant.

This concept can be expanded further to produce a wide variety of junction positions and shapes to tailor device performance as required. For example another phase shifter design investigated targeted polarisation independent operation. The phase efficiency for both TE and TM polarisations therefore must be the same. To achieve this a junction design with the flexibility to tailor the overlap of the depletion regions with the TE and TM modes was required. The design selected was a wrap-around junction as shown in figure 7.

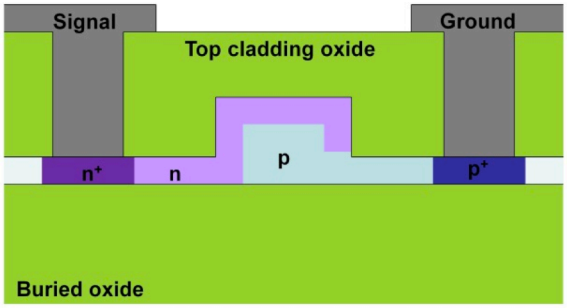


Fig. 7. Cross sectional diagram of the phase modulator design with wrap-around pn junction. The device is formed by a series of angled and straight self-aligned implants.

This design is formed with a series of self-aligned angled and vertical implants on either side of the waveguide to position the pn junction as required. The phase modulator in this case is formed in 400nm thick overlayer SOI to allow the formation of waveguide which support both polarisations. The waveguide height is therefore 400nm, the width 410nm and the slab height 100nm. The doping concentrations of the p and n type regions are designed to be approximately 1e18.cm$^{-3}$ whilst the doping concentrations of the highly doped regions are around 1e20.cm$^{-3}$. The phase modulators are inserted into asymmetric MZI with 80um arm length difference. Compact start couplers are used in this case to split and combine the light to and from the two MZI arms. The high speed operation of the device has been tested in a similar fashion as described for the previous device except that both polarisations are examined in this case. Open eye diagrams are obtained from the device at 10Gbit/s and 40Gbit/s (40Gbit/s eye diagrams shown in figure 8. At 10Gbit/s an extinction ratio of approximately 7.3dB is obtained for both polarisations [15]. At 40Gbit/s the extinction ratio drops slightly to 6.5dB but again is almost identical for both polarisations demonstrating the prospects for polarisation independent operation. An on chip insertion loss of ~25dB is obtained which comprises a device loss of ~15dB and the selection of a non-quadrature operating point which results in a further ~10dB of loss.

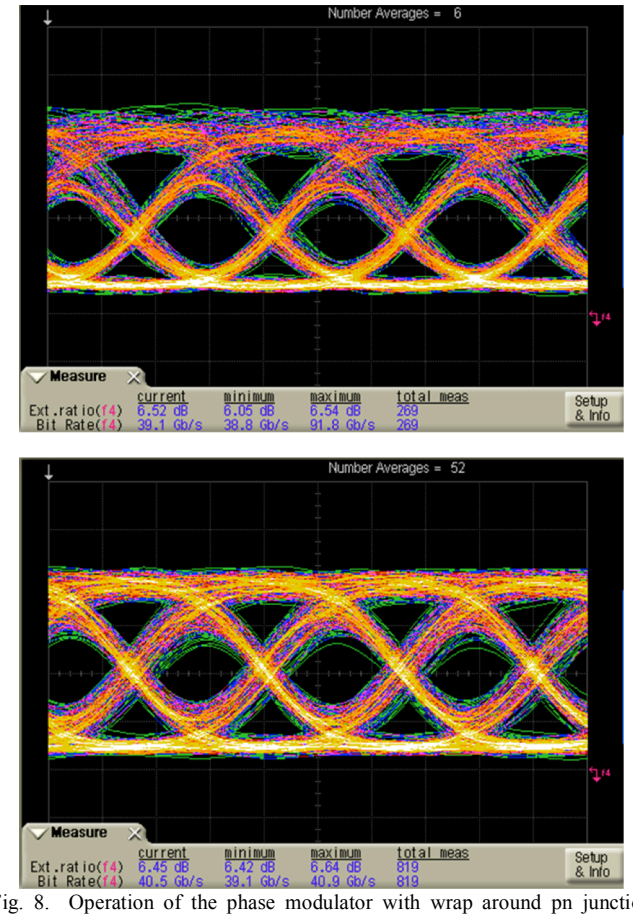


Fig. 8. Operation of the phase modulator with wrap around pn junction modulator at 40Gbit/s for TE polarisation (top) and TM polarisation (bottom). An almost identical extinction ratio of ~6.5dB is obtained in each case [15].

## III. Chirp Analysis

When transmitting data at high symbol rates over distances of tens of kilometres one important consideration is the chirp produced by the modulator. Chirp in optical intensity modulators is caused when the output phase of the light relative to the input phase changes with time. This causes a

slight excursion of the carrier wavelength during switching between the 1 and 0 states. This acts on the chromatic dispersion of the fibre causing a spreading or a compression of the pulse in time. The effect scales with propagation distance and therefore at certain distance pulses begin to overlap and the data becomes unresolvable unless a dispersion compensator is employed. In single-drive MZI devices, chirp is a common feature since as the relative phase of the active arm is varied with time to change the interference condition the relative phase of the resultant output will also change with time. In devices based upon the Pockels effect, chirp can theoretically be avoided by driving both arms of the MZI with complementary signals (commonly referred to as dual-drive or push-pull operation). In this case, provided that the optical power from each arm remains equal and the changing phase from either arm is equal but opposite, the output phase can be kept constant. In practice this should mean that the MZI splitters/combiners should provide precise 3dB behaviour, the optical losses in either arm are equal, the magnitude and timing of the drive signals to each arm are the same and the phase modulators in either arm are identical. A deviation from any of these conditions will cause some degree of chirp. As discussed above high speed optical modulators which are formed in silicon are most commonly based upon the plasma dispersion effect which relates changes in the free electron and hole densities to changes in refractive index and absorption coefficient. It is this unavoidable modulation of the material's absorption during modulation of the phase that causes a time dependant difference in the loss in either arm which is not equal because the carrier density in the two arms is instantaneously different causing differential absorption, and hence instantaneous imbalance. This problem is specific to all devices based upon this effect including plasma dispersion based silicon devices.

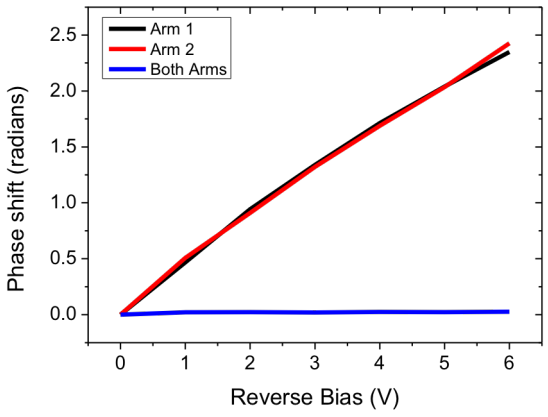


Fig. 9. Phase shift produced with different dc bias voltages for MZI arm 1 (black line), MZI arm 2 (red line), and the residual phase shift from when both MZI arms have the same DC voltage applied (blue line).

To analyse whether the degree of chirp produced by this cause is significant enough to prevent the consideration of silicon optical modulators for longer haul applications from the stand point of chirp a theoretical and experimental analysis has been performed on the device shown in figure 2. Analysis is performed for both single and dual drive operations. In the experimental analysis high speed ground-signal-ground-signal-ground (GSGSG) probes are used to apply the data signal to the device and to connect the DC block and 50Ω termination to the device. In single-drive operation (only one arm of the MZI is driven) a single output Centellax OA4MVM3 amplifier is used to boost the data signal up to 6.5V peak to peak. In dual-drive operation SAGE Laboritories OPS002 RF phase shifters are used to shift the timing of the complementary signals to the two arms to ensure that they are accurately aligned in time. A Centellax OA4SMM4 dual amplifier is then used to provide two complementary outputs of 3V peak to peak. A bias tee is used to apply a DC level to the signal to ensure that the device operates only in the depletion regime. In the dual-drive case the same DC level is applied to both arms.

In order to create an accurate model, the ratio of effective refractive index change $\Delta n_{eff}$ to absorption coefficient change $\Delta\alpha$ in the experimental device must be measured. To measure the change in phase with voltage, one arm of the asymmetric MZM was grounded and a DC voltage applied to the other. The spectral shift of the MZM's response was then measured with different voltage levels and converted to phase shift as described previously. Due to the self-aligned process used to fabricate the device, variations in performance between the two MZI arms due to misalignment are eliminated. Experimental measurements have confirmed that a near identical phase shift was observed from the two MZM arms as shown in figure 9.

To measure the change in absorption coefficient the same DC level was applied to both MZI arms simultaneously and the shift in the power level of the MZI response was observed for different bias voltages. Any significant mismatch in the phase shifting performance of the modulators would produce a phase shift at the output of the MZI. The blue line in figure 9 indicates any phase shift difference is negligible. The change in effective refractive index and absorption coefficient with voltage is shown fig. 10. This relationship is used to calculate the effective changes in electron and hole densities during modulation which are then used in the chirp model.

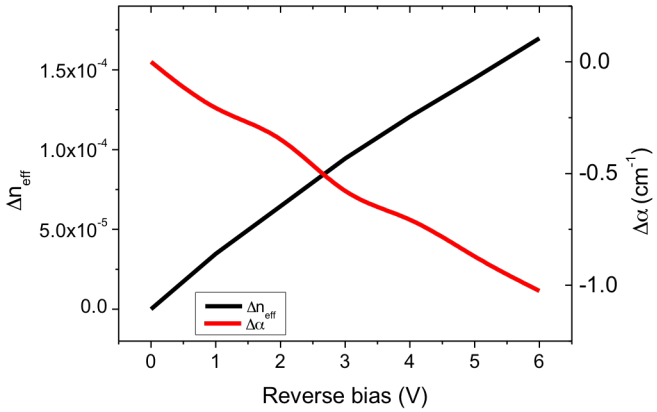


Fig. 10. Relationship of effective refractive index change and absorption change with different reverse bias voltages.

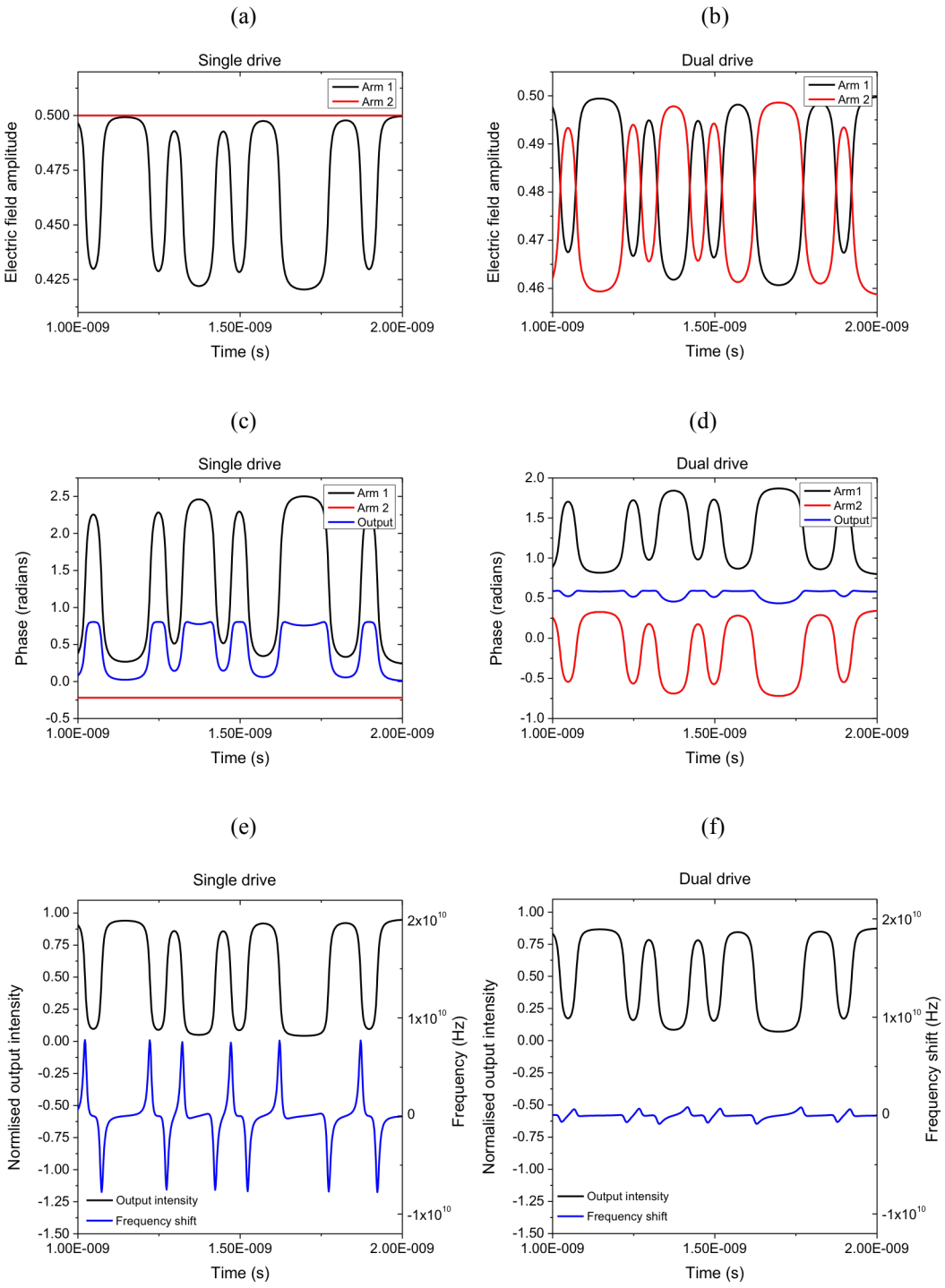


Fig. 11. Simulation data. Optical electric field amplitude in each MZI arm against time for single drive operation (a) and dual drive operation (b). Phase of the light in each arm and at the modulator output relative to the input against time for single drive operation (c) and dual drive operation (d). Modulator output intensity and frequency shift against time for single drive (e) and for dual drive (f).

The high speed response of the device and drive circuitry is also important as it defines the rate at which the output phase changes during modulation. Optical eye diagrams were obtained from which the rise and fall times of 20ps (single drive) and 24ps (dual drive) were measured. These figures were also taken into account in the device model. A data rate of 20Gbit/s is used in order to capture a good number of data points per transition on the optical modulation analyser used for the chirp measurements that will be described below.

To analyse the degree of chirp produced, a computer model representing the silicon modulator has been developed. An input non return to zero (NRZ) PRBS data stream at 20Gbit/s is defined with the same rise and fall times as those produced experimentally. In order to isolate the cause of chirp specific to silicon optical modulators, the computer model assumes equal power splitting, equal arm losses and in the dual drive

case equal but opposite phase changes in either arm. These assumptions are not invalid. A passive extinction ratio of around 30dB has been demonstrated from the MZI as shown in figure 3. This indicates a well-balanced optical power at the output of either arm. Furthermore the negligible difference has been observed in the performance of the phase modulators in either arm (figure 9). The DC characteristics which describe the ratio of refractive index change to absorption change in the experimental case have been put into the model to correctly represent the silicon modulator. The degree of modulation applied in the simulation is used to match experimental extinction ratio. The top two plots of figure 11 show how the electric field amplitude of the optical wave at the output of either arm of the MZI changes during modulation for the single drive and dual drive cases respectively. The output phase of the modulator will tend toward the phase of the arm with the greater optical power. Since the ratio of the electric field amplitude from each arm is changing with time due to the time dependent losses, it is not possible to keep a constant output phase even if the phase change in each arm is equal and opposite. This is demonstrated in the middle two plots of figure 11 showing the phase from each of the MZI arms and the MZI output phase relative to the input phase with time. It can be seen in both the single drive and dual drive cases that the output phase relative to the input phase is not constant with time. In reality this means that the phase of the light is changing faster or slower than in the unmodulated case which therefore causes a shift of the carrier frequency. Finally this frequency shifting resultant from the change in relative phase is shown against time in both cases together with the MZI output intensity in the bottom two plots of figure 11. In the dual drive case the peak frequency shift is around 0.5GHz whereas for the single drive case the frequency shift is in excess of 7.5GHz. The effective chirp parameter as used in [6] can be misleading for this type of modulator since theoretically it will be ~zero when the device is operated with the "1" level at the maximum of the MZI response, with precise splitting and with equal (but opposite) modulation in either arm. In this case the relative output phase at the "1" level and at quadrature is approximately equal. There will however be movement of the relative output phase outside of these two states causing some degree of frequency chirping as demonstrated in figure 11. However, to allow comparison with [6], the effective chirp parameter has been calculated in the same way to be -1.7 for the single drive case and near zero for dual drive case. To experimentally analyse the modulator for chirp and to verify the theoretical model the output signal from the modulator was characterised using an optical modulation analyser (OMA, Agilent N4391A), in conjunction with an 80GSa/s real-time oscilloscope (Agilent DSO-X 93204A). An OMA is capable of analysing a complex signal and offering constellation analysis. The experimental setup and conditions are described in [16]. The wavelength used during these measurements was 1549.4nm at which the modulator operates at quadrature. Figure 12 shows the experimental constellations of the modulation for both modes of operation. The simulated constellation from the modulator model is also overlaid. The minimum has been set to (0,0) and maximum normalised to position (1,0) on the constellation in both experimental and simulated data to allow for ease of comparison. Due to a poor signal-to-noise ratio at the output of the EDFA the transitions between the 1 and 0 levels appear blurred in the measured constellation diagram.

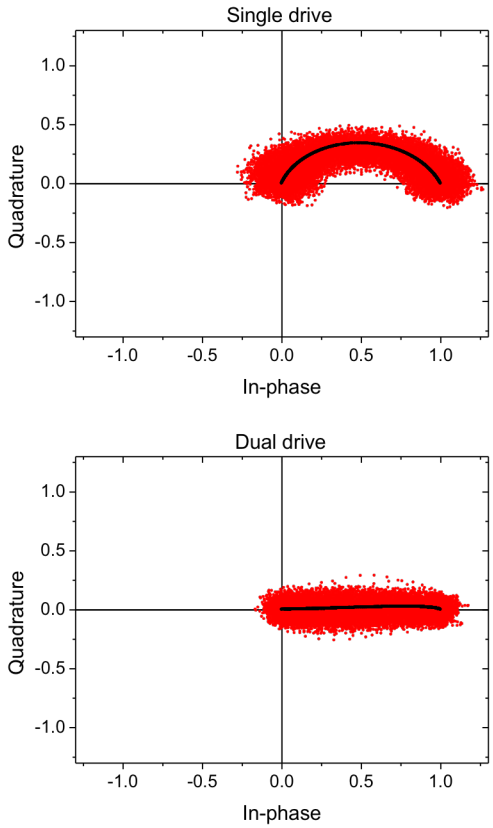


Fig. 12 Experimental (red points) and theoretical (black line) constellation diagrams measured with OMA for single drive operation (top) and dual drive operation (bottom).

The constellation plots display both the phase and normalised amplitude of the modulator output in vector format. The x-axis represents the in-phase component (output light in-phase with input light) and the y-axis represents the quadrature component (output light $\pi/2$ out of phase from the input light). A straight transition between the 0 and 1 levels indicates that the output phase is not changing during modulation and therefore that there is zero chirp. In the dual drive case the transition between the 1 and 0 levels is nearly straight confirming a low level of chirp. In the single drive case a curved transition is observed. This indicates a chirped output since significant deviation of the output phase is occurring during modulation, as predicted by the theoretical model. It can be seen that in both modes of operation there is a good agreement between the measured and modelled data. Using the theoretical level of chirp predicted in the model we are able to predict its impact on the long haul transmission of data. Our calculations show that the pulses formed in the dual drive case propagate similarly to totally unchirped pulses, confirming that the chirp under this driving configuration is negligible. This is consistent with the findings of others

analysis [7]. Chirp is also present in the output of typical ring resonator based optical modulators due to the non-constant phase response of the ring around its resonance at which it is operated for intensity modulation. It has been proposed that more complex structures can be used to eliminate chirp [17] and that in certain modes of operation negative chirp can be engineered to facilitate propagation over longer distances of fibre [18].

## IV. Large Dynamic Extinction Ratio

To demonstrate the ability of a silicon optical modulator to produce a large dynamic extinction ratio as also required for longer haul applications a MZM with 3.5mm long phase modulators of efficiency ~2.3V.cm were employed. With this efficiency, phase modulator length and a 6.5V peak to peak drive voltage a full pi phase shift is achievable. The spectral response of the MZI at different DC voltages is shown in figure.13.

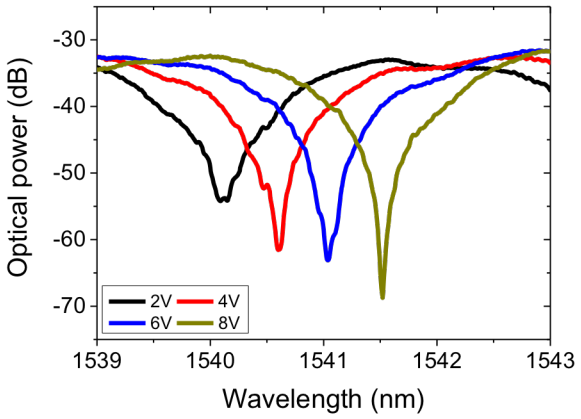


Fig. 13 Spectral response of the MZI with 3.5mm long phase modulators of 2.3V.cm efficiency at different DC voltages.

During high speed experiments a 5V DC bias was used together with the 6.5V drive which gives a voltage swing from 1.75V to 6.25V. Over this range of voltages at a wavelength around 1541.5nm a DC modulation depth in excess of 30dB is achievable.

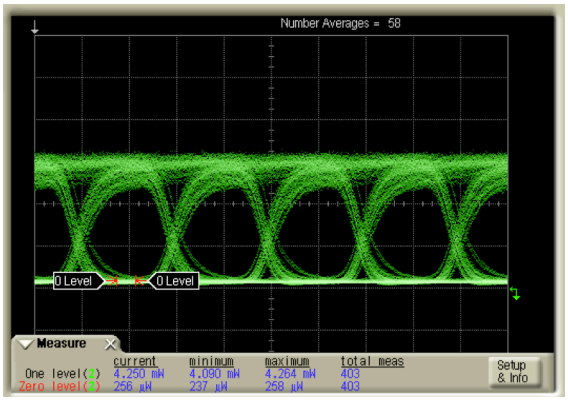


Fig. 14 Optical eye diagram at 10Gbit/s with 18dB modulation depth

A 10Gbit/s PRBS data stream was produced using a Centellax TG2P1A source and amplified to 6.5V peak to peak using a Centellax OA4MVM3 amplifier. This was applied to the device using GSG probes. The output light from the device was amplified using an Alnair Labs LNA 150 EDFA. The light was then filtered to attenuate to some extent the noise from surrounding wavelengths which is produced by the EDFA and then passed to an Agilent 86100C digital communications analyser with 86116C Opt 40 optical head. The resultant eye diagram is shown in figure 14. When residual EDFA noise of 190uW is subtracted from the 1 and 0 levels an extinction ratio of approximately 18dB results.

## Summary

Different variants of high performance silicon optical modulators built by self-aligned processes have been presented. A MZM based in 220nm thick overlayer SOI has demonstrated operation up to 50Gbit/s and at 40Gbit/s with an extinction ratio of 10dB and optical loss of 15dB. It has been shown that the optical loss of the phase modulator in this case can be decreased from 4dB/mm to 1.1dB/mm by slightly increasing the separation of the highly doped regions from the waveguide. The chirp produced when the device is driven in both single and dual drive configuration has been analysed. It has been shown that the chirp produced is negligible when the device is operated in the dual drive configuration. Also presented is a higher efficiency version of the device operating at 10Gbit/s with a dynamic extinction ratio of ~18dB. This data demonstrates that silicon modulators can satisfy some of the specifications required for long haul communications, and that they have the potential for further optimisation to produce low cost alternatives to current devices. Finally a second MZM modulator fabricated in 400nm thick overlayer SOI has demonstrated 40Gbit/s operation for both TE and TM polarisations showing the potential for a polarisation independent device.

## References

[1] C. E. Png, S. P. Chan, S. T. Lim and G. T. Reed, "Optical phase modulators for MHz and GHz modulation in silicon-on-insulator (SOI)," Journal of Lightwave Technology, vol. 22, pp. 1573-1582, 2004

[2] D. J. Thomson, F. Y. Gardes, J-M. Fedeli, S. Zlatanovic, Y. Hu, B. P. P. Kuo, E. Myslivets, N. Alic, S. Radic, G. Z. Mashanovich, and G. T. Reed, "50-Gb/s silicon optical modulator," IEEE Photon. Technol. Lett **24**(4), 234-236 (2012).

[3] P. Dong, L. Chen, and Y-k. Chen "High-speed low-voltage single-drive push-pull silicon Mach-Zehnder modulators" Opt. Express, **20**(6), 6163-6169, (2012).

[4] www.luxtera.com

[5] Y. Wei, Y. Zhao, J. Yang, M. Wang, and X. Jiang "Chirp characteristics of silicon Mach-Zehnder modulator under small-signal modulation," IEEE J. Lightwave Technol. **29**(7), 1011 – 1017, (2011)

[6] L. Chen, P. Dong, and Y-K. Chen, "Chirp and dispersion tolerance of a single-drive push-pull silicon modulator at 28Gb/s," IEEE Photon. Technol. Lett. **24**(11), 936-938, (2012).

[7] K. Goi, K. Oda, H. Kusaka, Y. Terada, K. Ogawa, T-Y. Liow, X. Tu, G-Q. Lo, and D-L. Kwong "11-Gb/s 80-km transmission performance of zero-chirp silicon Mach–Zehnder modulator," Opt. Express, **20**(26), B350-B356, (2012).

[8] http://www.photline.com/filer/get/14/ReviewModulSpecs.pdf

[9] http://dev.oclaro.com/product_pages/Powerbit_F10-0.php

[10] J. Ding, H. Chen, L. Yang, L. Zhang, R. Ji, Y. Tian, W. Zhu, Y. Lu, P. Zhou, and R. Min , "Low-voltage, high-extinction-ratio, Mach-Zehnder

silicon optical modulator for CMOS-compatible integration," Opt. Express, **20**(3), 3209-3218, (2012).
[11] R. A. Soref, and B.R. Bennett, "Electrooptical Effects in Silicon," IEEE J. Quantum Elect., vol. QE-23, pp. 123-129, 1987.
[12] M. Nedeljkovic, R. Soref, and G. Z. Mashanovich, "Free-carrier electro-refraction and electro-absorption modulation predictions for silicon over the 1-14um infrared wavelength range," IEEE Photonics J. **3**(6), 1171 – 1180, (2011).
[13] D. J. Thomson, F. Y. Gardes, Y. Hu, G. Mashanovich, M. Fournier, P. Grosse, J-M. Fedeli and G. T. Reed, "High contrast 40Gbit/s optical modulation in silicon," Opt. Express, 19(12), 11507 – 11516, (2011).
[14] D. J. Thomson, Y. Hu, G. T. Reed, J-M. Fedeli, "Low loss MMI couplers for high performance MZI modulators," Photonics Technology Letters, 22(20), 1485-1487, (2010).
[15] F. Y. Gardes, D. J. Thomson, N. G. Emerson, and G. T. Reed, "40 Gb/s silicon photonics modulator for TE and TM polarisations," Opt. Express, 19(12), pp. 11804-11814, 2011
[16] S. Liu, D. J. Thomson, F. Y. Gardes, J-M. Fedeli, P. Petropoulos, and G. T. Reed, "Characterization of the chirp of silicon optical modulators," European Conference and Exhibition on Optical Communication (ECEOC) Tu.1.E.5, (2012).
[17] T. Ye, Y. Zhou, C. Yan, Y. Li and Y. Su, "Chirp-free optical modulation using a silicon push-pull coupling microring," Optics Letters, 34(6), pp.785-787, (2009).
[18] L. Zhang, Y. Li, J-Y. Yang, M. Song, R. G. Beausoleil and A. E. Willner, "Silicon-Based Microring Resonator Modulators for Intensity Modulation," IEEE Journal of Selected Topics in Quantum Electronics, 16(1), pp. 149-158, (2010).

**David J. Thomson** is a senior research fellow in the Optoelectronics Research Centre (ORC) at the University of Southampton. His research interests are optical modulation, optical switching, integration and packaging in silicon. He started his silicon photonics research in 2004 as a PhD student at the University of Surrey under the guidance of Prof. Graham Reed. His PhD project involved investigating silicon based total internal reflection optical switches and more specifically methods of restricting free carrier diffusion within such devices. In 2008 he took up a role as a research fellow in the same research group leading the work package on silicon optical modulators within the largest European silicon photonics project named HELIOS. Within this project David designed the first silicon optical modulator operating at 50Gbit/s. In 2011 David presented invited talks at SPIE Photonics West and IEEE Group IV Photonics conferences and in 2012 was selected to present his work at the SET for Britain event in the Houses of Parliament.

**Frederic Y. Gardes** is an Academic Fellow appointed as a lecturer at the University of Southampton in the Electronics and computer science department (ECS); he is conducting his research as part of the Optoelectronics Research Centre (ORC). Gardes previous research covers silicon photonics and particularly high speed active optical devices in silicon and germanium. In 2005 Gardes initiated work on silicon optical depletion modulators and was the first to predict operation above 40GHz. In 2011 Gardes and his collaborators demonstrated optical modulation of up 50 Gb/s and a 40Gb/s modulator with a quadrature Extinction Ratio (ER) of 10dB setting a new state of the art performance in both speed of modulation in silicon devices and extinction ratio. Gardes is currently working with several national and international collaborators in two large research programs where he leads the research effort in optical modulators and detector integration. These programmes are the £5M UK Silicon Photonics project funded by EPSRC, and the £8M EU FP7 HELIOS. Gardes is also involved in photonic crystal slow light, ultra-low power nano-cavity modulators, Silicon/Germanium QCSE devices, Germanium and defect induced detectors in silicon and active device integration in group IV materials. Gardes has authored more than 80 publications and 5 book chapters in the field of Silicon Photonics. He has also been involved in the FP6 ePIXnet program and is a regular invited and contributing author to the major Silicon Photonics conferences around the world. Gardes is also a member of the programme committee of the IEEE Group IV Photonics conference.

**Sheng Liu** received the B.Eng. degree in electronics from Tsinghua University, Beijing, China, in 2005, and the M.Sc. degree in electronics from the University of Southampton, Southampton, U.K., in 2007. He obtained his PhD from the University of Southampton working within the Optoelectronics Research Centre. His research interests include on all-optical signal processing in nonlinear waveguides.

**Henri Porte** has over 25 years of extensive experience in Optoelectronics and Telecommunications. Before becoming a founding member of Photline Technologies in 2000, Dr. Porte was a Senior Scientist at the CNRS (National Scientific Research Centre), followed by a position as the Director of Research and Head of the Optoelectronics Group at the Optics Laboratory of the University of Besançon. Dr. Porte has authored or co-authored more than 100 publications in journals and international conferences and holds 14 patents. In charge of executive in Photline Technologies, he manages the strategic orientations and the innovative and scientific policies

**Lars Zimmermann** joined IMEC in 1998, and received his joint PhD from Katholieke Universiteit Leuven & IMEC in 2003 for his work on near-infrared sensors comprising the technology chain from layer growth to flip-chip integration. In 2004, he joined TU Berlin, where he worked on Silicon waveguide and optical motherboard technology. Since 2006, he has been the coordinator of the Photonic Packaging Platform. In 2008 he joined IHP. Since then, he is the scientific head of the Joint Lab Silicon Photonics between IHP & TU Berlin, and is responsible for photonics technology development at IHP. He teaches a one semester course on Silicon Photonics at TU Berlin.

**Jean-Marc Fedeli** received his electronics engineer diploma from INPG Grenoble in 1978. Then he conducted researches at the CEA-LETI on various magnetic memories and magnetic components as project leader, group leader, and program manager. For two years, he acted as advanced program director in Memscap company for the development of RF-MEMS, then he returned to CEA-LETI in 2002 as coordinator of silicon photonic projects up to 2012. Under a large partnership with universities and research laboratories, he works on various technological aspects on Photonics on CMOS (Si rib and stripe waveguides, $Si_3N_4$ and a-Si waveguides, slot waveguides), Si modulators, Ge photodetectors, SiOx material, InP sources on Si. His main focus is on the integration of a photonic layer at the metallization level of an electronic circuit. He has been participating on different European FP6 projects (PICMOS, PHOLOGIC, MNTE, ePIXnet). Under the European FP7, he was involved in the WADIMOS ,PhotonFAB (ePIXfab) projects and was program manager of the HELIOS project. He is currently managing the FP7 PLAT4M project on Silicon Photonics Platform and involved in a CELTIC project as well as industrial projects on Silicon Photonics. His H factor is around 20 with more than 150 publications and 50 patents. He wrote three book chapters (one on magnetic recording and two on silicon photonics).

**Youfang Hu** was awarded the degree of BEng in Optoelectronics, Tianjin University, China, in June 2001. He moved to the UK for PhD study at Aston University, Birmingham, UK, in Oct 2001. The research in his PhD was focused on ultrafast diode lasers. He was awarded PhD degree in July 2005. He worked as a computational physicist in Photon Design, Oxford, UK from 2005-2007. Then he joined the Optoelectronic Research Centre, University of Southampton, UK in July 2007 as a research fellow. From Jun 2009 to date, he is a research fellow in the Silicon Photonics Group, University of Surrey/Southampton. Currently, his research covers a variety of topics, including passive silicon photonic devices, e.g. WDMs, wavelength filters and surface grating couplers, QCSE photodetectors/modulators, silicon photonics integration, and nano-fabrication technology.

**Milos Nedeljkovic** received the M.Eng. degree in communications engineering from the University of Durham, UK in 2009. He is currently working towards a Ph.D. degree at the University of Southampton, Southampton, UK. His research interests include Group-IV material photonics for mid-infrared wavelengths, and modulation mechanisms in silicon.

**Xin Yang** was born in Nanchang, China. He received the BSc degree in physics from Shanghai University, Shanghai, China, in 2006, and received the MSc degree in Radio Frequency Communication Systems from University of Southampton, Southampton, UK in 2008. He is currently working toward the Ph.D. degree in Optical Communications in the Optoelectronics Research Centre, University of Southampton, Southampton, UK. His current research interests include the nonlinear optical signal processing for optical fibre communication applications, ultra-fast fibre lasers and etc. Mr. Yang is a student member of the Optical Society of America.

**Periklis Petropoulos** graduated from the Department of Electrical Engineering and Information Technology, University of Patras, Greece in 1995. He received the MSc degree in Communications Engineering from the University of Manchester Institute of Science and Technology, UK in 1996 and the PhD degree in Optical Telecommunications from the Optoelectronics

Research Centre (ORC), University of Southampton, UK in 2000. Dr. Petropoulos is a Professor of Optical Communications at the ORC. His research interests lie in the fields of optical communications, all-optical signal processing and nonlinear fibre technology. He has participated in several European Union and national research projects in the field of optical communications. His research has produced more than 330 papers in technical journals and conference proceedings, including several invited and post-deadline papers in major international conferences, and holds 6 patents. Dr. Petropoulos is a Senior Member of the Optical Society of America. He has served as member of the Technical Programme Committees for several international conferences, including the European Conference on Optical Communication (ECOC), the Optical Fiber Communication (OFC) conference and the European Conference on Lasers and Electro-optics (CLEO/Europe).

**Goran Z. Mashanovich** received Dipl. Ing. and MSc in Optoelectronics from the Faculty of Electrical Engineering, University of Belgrade, and PhD in Silicon Photonics from the University of Surrey. Since 2000, he has been a member of the Southampton Silicon Photonics Group, and his is actively researching near- and mid-infrared photonic devices in group IV materials. Dr Mashanovich has published 140 papers in the field and is a member of several international conference committees related to photonics.